

**Title:** Theta oscillations integrate functionally segregated sub-regions of the medial Prefrontal Cortex

**Authors:** Ernest Mas-Herrero<sup>1,2</sup>, Josep Marco-Pallarés<sup>1,3</sup>

**Affiliations:**

1. Cognition and Brain Plasticity Group [Bellvitge Biomedical Research Institute – IDIBELL], L'Hospitalet de Llobregat, Barcelona, 08097, Spain
2. Montreal Neurological Institute, McGill University, Montreal, QC H3A 2B4, Canada
3. Department of Cognition, Development and Psychology of Education, Institute of Neurosciences, University of Barcelona, Barcelona, 08035, Spain.

**Corresponding Author:** Josep Marco-Pallarés

Department of Basic Psychology - IDIBELL

L'Hospitalet de Llobregat,

University of Barcelona, Campus Bellvitge,

Barcelona 08097, Spain

Tel: +34 934020993

e-mail: [josepmarco@gmail.com](mailto:josepmarco@gmail.com)

## **ABSTRACT**

Reinforcement learning requires the dynamic interplay of several specialized networks distributed across the brain. A potential mechanism to establish accurate temporal coordination among these paths is through the synchronization of neuronal activity to a common rhythm of neuronal firing. Previous EEG studies have suggested that theta oscillatory activity might be crucial in the integration of information from motivational and attentional paths that converge into the medial Prefrontal Cortex (mPFC) during reward-guided learning. However, due to the low spatial resolution of EEG, this hypothesis has not been directly tested. Here, by combining EEG and fMRI, we show that theta oscillations serve as common substrate for the engagement of separated sub-regions within the mPFC (the pre-Supplementary Motor Area and the dorsomedial Prefrontal Cortex), underlying different cognitive operations (encoding of outcome valence and unsigned prediction errors) through separate functional paths (the Salience and the Central Executive Networks).

**Keywords:** Reward processing, theta oscillations, medial Prefrontal Cortex, Reinforcement learning

## INTRODUCTION

One of the most challenging tasks that people have to face in their everyday life is to rapidly and accurately adapt their behavior based on current outcomes and previous experiences. An essential element for successful goal-directed behavior is to continuously monitor the context, the predictive relation between events, and the value of outcomes in order to derive appropriate cognitive, affective, and behavioral adaptations. In order to accomplish this, the brain has to integrate information from several specialized networks, involved, among others, in attention and motivation. In that sense, brain regions containing converging terminals from these networks might represent key nodes for the integration of information across these functional paths. One of these structures is the medial Prefrontal Cortex (mPFC), which encompasses the supplementary motor area (SMA) and pre-SMA and extends rostrally along the dorsomedial prefrontal cortex (dmPFC) among other cortical areas (Ridderinkhof et al., 2004; Ullsperger et al., 2014). This large and heterogeneous cortical region has extensive connections with other parts of the brain involved in cognitive control and motivation among others, and has been related to the monitoring of diverse dimensions of outcome-processing such as value, surprise, risk or uncertainty (Ridderinkhof et al., 2004; Ullsperger et al., 2014). Based on this evidence, the mPFC might represent a key node to integrate information across different functional networks with the objective of performing attentional and behavioral adjustments according to environmental demands.

However, in order to establish efficient communication, functional networks converging in the mPFC (such attentional or motivational networks) need to be engaged into a common temporal context in which they can interact and influence each other. The synchronization of neuronal activity to a common rhythm of neuronal firing might be an ideal functional mechanism to establish such accurate temporal coordination among different regions and networks (Buzsáki and Draguhn, 2004; Womelsdorf et al., 2007). This synchronous activity gives rise to fluctuating local

field potentials that can be recorded on the surface of the scalp by means of electroencephalography (EEG) recordings. Under this context, previous EEG studies have identified an oscillatory component – mid-frontal theta oscillatory activity (4-8 Hz) – which has been suggested to play an important role in outcome monitoring processes (Cohen et al., 2011). In particular, this oscillatory activity has been shown to be sensitive to, at least, two different aspects of outcome monitoring: evaluation of the valence and the unexpectedness of the outcome or unsigned prediction errors (Mas-Herrero and Marco-Pallarés, 2013). These two features of feedback evaluation have been suggested to reflect either motivational or attentional functions of the mPFC (Cavanagh et al., 2011; Mas-Herrero and Marco-Pallarés, 2013). In fact, recent studies have pointed out that mid-frontal theta oscillations could be a common substrate for action monitoring processes; providing a temporal template for the coordination of the different networks engaged in the mPFC (Cavanagh et al., 2012). However, due to the low spatial resolution of EEG, it remains unknown to what extent the dynamics of this signal are reflecting the engagement of one single sub-region or in contrast, it reflects the simultaneous recruitment of several specialized sub-regions of the mPFC involved in different cognitive operations.

In order to study this relationship, seventeen participants were involved in both EEG and fMRI experiments in which subjects were engaged in a reversal learning task in two separate sessions. In such task, participants have to constantly monitor the outcome of their choices in order to adapt to potential changes in the environment, as action contingencies are reversed after certain number of trials. We aimed to understand to what extent the modulation of mid-frontal theta oscillations with outcome valence and unsigned prediction errors (UPE) underlie the engagement of one single sub-region of the mPFC, encoding both processes; or in contrast, theta rhythms synchronize the action of different sub-regions of the mPFC involved in different cognitive operations, providing a temporal template for the integration of such computations.

## MATERIALS AND METHODS

**Participants.** Seventeen students from the University of Barcelona ( $M = 21.8$  years,  $SD = 2.5$ , 7 males) participated in the experiment. All participants were paid 10€ per hour and a monetary bonus depending on their performance. All participants gave written informed consent, and all procedures were approved by the local ethics committee.

**Experimental procedure.** Each participant performed a reversal learning task (Cools et al., 2002) in two separated sessions. One in which EEG data was recorded and a second one, four months later, in which functional images were acquired.

In the EEG session, the task consisted of 637 trials divided into 49 blocks (10 to 16 trials each). Figure 1 shows the task design. In each trial, two geometric figures (a square and a triangle) were presented on either side of a central fixation point. The participants were instructed to select the square or the triangle by pressing a corresponding button (left or right) with his/her index and middle finger during the presentation of the figures. The position of the figures (left or right) was randomized in each trial. After a delay of 1000 ms, one of two possible types of feedback was displayed: a green tick (reward, +€0.04) or a red cross (punishment, -€0.04). Feedback remained on the screen for 1000 ms. and a new trial was presented after a delay of 750 ms. On each block, one figure was rewarded in 75% of the trials and punished in the 25% of the trials, while the other was rewarded in 25% of the trials and punished 75% of the trials (Figure 1). However, at the beginning of each block, and without informing the participant the rule was reversed. Note that participants may not fully predict the occurrence of a reversal as the stimuli were the same for all the blocks (see Figure 1) and the length of each block varied randomly from 10 to 16 trials. Similar approaches have been extensively used in the literature (Cools et al., 2002, Fellows and Farah, 2003, Cools et al., 2007, Jocham et al., 2009, Philiastides et al., 2010; Chase et al., 2011, Padrao et al., 2015). However, to facilitate the reversal, during the first five trials following the

contingency reversal, a selection of the previously correct stimulus resulted in punishment. All the trials were included in further behavioral and EEG analysis except those trials in which the participants did not respond in the requested time (1000 ms), which were discarded from further analysis. In case of late response, a question mark appeared on the screen after the stimuli. Self-paced rest periods were given after 35-40 trials. During these pauses, the participants were told how much money they had earned up to that point.

In the fMRI session, the task consisted of three runs of 104 trials each divided into 8 blocks (10 to 16 trials each). The paradigm used in the fMRI session was the same as in the EEG session except that cues were presented after a variable interval (randomly jittered among 300, 800, 1500 and 2300 ms) and the inter-trial duration was variable to set the duration of the trial to 5000 ms. These modifications were applied to adapt to the different technical requirements of each neuroimaging modality. We used standard number of trials for both fMRI (our task had 312 trials -104 trial per run; similar to Cools et al., 2002 or Jocham et al., 2009) and EEG (our task had 637 gains and losses; similar to Mas-Herrero and Marco-Pallares, 2013, Chase et al., 2011 or Philiastides et al., 2010).

The participants were encouraged to earn as much money as possible in both sessions.

**Reinforcement Learning Model.** A Q-learning model (Watkins and Dayan, 1992) was implemented using the data from both sessions. The model used reward prediction error to update the weights associated with each stimulus and probabilistically chose the stimulus with the higher weight. The weights are updated using the following algorithm:

$$V(a)_t = V(a)_{t-1} + \alpha\delta$$

where  $\alpha$  is the learning rate and  $\delta$  represents the prediction error, calculated as the difference between the outcome and the expectancy or weight of the selected figure. Next, softmax action selection was used to compute the probability of choosing one of the two options:

$$p(a) = \frac{e^{V(a)\gamma}}{e^{V(a)\gamma} + e^{V(b)\gamma}}$$

where  $\gamma$  is the inverse of the temperature.  $\gamma$  determines the degree with which differences in reward values between two potential actions are translated into a more deterministic choice.

The model was run ten times, using random initial values for each subject by maximizing the log likelihood estimate (LLE) with the the `fmincon` function of Matlab R2008. The parameters  $\alpha$  and  $\gamma$  with the best log likelihood estimate were selected. Once  $\alpha$  and  $\gamma$  were individually calculated, values representing the prediction error could be determined on a trial-by-trial basis.

**Electrophysiological recording.** EEG was recorded from the scalp (band-pass filter: 0.01 – 250 Hz, with a notch filter at 50 Hz; 500 Hz sampling rate) using a BrainAmp amplifier (Brain Products GmbH) with tin electrodes mounted in an electrocap (Electro-Cap International) located at 29 standard positions (Fp1/2, Fz, FCz, F7/8, F3/4, Fc1/2 Fc5/6, Cz, C3/4, T3/4, Cp1/2, Cp5/6, Pz, P3/4, T5/6, PO1/2, Oz) and the left and right mastoids. An electrode placed at the lateral outer canthus of the right eye served as an online reference. EEG was re-referenced off-line to the linked mastoids. Vertical eye movements were monitored with an electrode at the infraorbital ridge of the right eye. Electrode impedances were kept below 5 k $\Omega$ . Trials with absolute mean amplitudes higher than 100  $\mu$ V were automatically rejected off-line. Additionally, we performed a carefully visual inspection of the remaining trials after this automatic rejection. As a result, 10.5% (SD = 9.1) of the trials were rejected (Gains: M = 9.3%, SD = 8.9; Losses: M = 12.4%, SD = 9.8).

**EEG analysis.** Time-frequency analysis was performed per trial in 4 second epochs (2 seconds prior to feedback through to 2 seconds after) using 7-cycle complex Morlet wavelets. Changes in time-varying energy (square of the convolution between wavelet and signal) in the studied frequencies (1 to 30 Hz, in steps of one) were computed for each trial in all channels. In order to compare different conditions, trials associated with a specific condition were averaged for each subject and baseline corrected before performing a grand average. For trial-by-trial analysis, changes in time-varying energy in the studied frequencies with respect to the average baseline (100 ms before feedback onset) were computed for each trial.

To study the relationship between mid-frontal theta activity and both outcome valence and unsigned prediction error, negative and positive feedback were independently sorted into ten bins according to the size of the absolute reward prediction error (the 10<sup>th</sup>, 20<sup>th</sup>, 30<sup>th</sup>, 40<sup>th</sup>, 50<sup>th</sup>, 60<sup>th</sup>, 70<sup>th</sup>, 80<sup>th</sup>, 90<sup>th</sup> and 100<sup>th</sup> percentile of the range).

For all statistical effects involving two or more degrees of freedom in the numerator, the Greenhouse-Geisser epsilon was used as needed to correct for possible violations of the sphericity assumption. The p-values following correction are reported.

Finally, a multiple-regression analysis was performed using unsigned prediction error and outcome valence as predictors of mid-frontal theta power (4-8 Hz, 200-400 msec.). We then determined whether the values of the slopes were different overall from 0 for the group using a one-sample t test. A significant difference from 0 would suggest a relationship between both effects and increases of mid-frontal theta activity. We used these beta values as index of the impact of both variables on participant's mid-frontal theta power increases to further analyze their relationship with the fMRI data.

**fMRI recording.** fMRI data was collected using a 3T whole-body MRI scanner (General Electric MR750 GEM E). Conventional high-resolution structural images [magnetization-prepared rapid-acquisition gradient echo sequence, repetition time (TR) = 4.7 ms, echo time (TE) = 4.8ms, inversion time 450 ms, flip angle 12°, 1 mm thickness (isotropic voxels)] were followed by functional images sensitive to blood oxygenation level-dependent contrast (echo planar T2\*-weighted gradient echo sequence, TR=2000 ms, TE=35 ms, flip angle 90°). Each functional run consisted of 270 sequential whole-brain volumes, comprising 30 axial slices aligned to the plane intersecting the anterior and posterior commissures, 3.5 mm in-plane resolution, 4 mm thickness, no gap, positioned to cover all but the most superior region of the brain and the cerebellum.

**fMRI Analysis.** Preprocessing was carried out using Statistical Parametric Mapping software (SPM8, Wellcome Department of Imaging Neuroscience, University College, London, UK, [www.fil.ion.ucl.ac.uk/spm/](http://www.fil.ion.ucl.ac.uk/spm/)). Additionally, image volumes with significant motion artifact were identified using the ArtRepair toolbox based on scan-to-scan motion (head position change exceeding 0.5 mm or global mean BOLD signal change exceeding 1.3%) and replaced by linear interpolation between the closest non-outlier volumes. From the 810 volumes acquired for each participant, on average, 1.1% (SD = 1.9) were corrected.

Functional images were first sinc interpolated in time to correct for slice timing differences and realigned. Realigned images were then spatially smoothed with a 4 mm FWHM kernel before they were motion-adjusted by ArtRepair toolbox. The corrected images were co-registered to the mean EPI image and normalized to the ICBM152 standard template in Montreal Neurological Institute (MNI) space. Finally images were spatially smoothed with a 7 mm FWHM kernel.

For the statistical model an event-related design matrix was specified using the canonical hemodynamic response function. Three regressor onsets were included for each trial: cue, response and feedback event. Response regressor also contained a parametric regressor indicating

whether the response was done with the index (value of 1) or the middle finger (value of 0). Finally, feedback regressor had two parametric regressors associated, variations in unsigned prediction error derived from the RL model and the outcome valence (with losses indicated with 1 and gains as 0). At first-level, outcome valence and unsigned prediction error contrasts were specified for all subjects as each condition against the implicit baseline. These contrast images were introduced into a second level t-test analysis. All results from the fMRI analysis are shown at a FWE corrected  $p < 0.05$  value at peak-level with a minimal cluster size of 2 voxels.

**ROI Analysis.** In order to assess the relationship between brain responses in outcome valence- and UPE-sensitive regions and mid-frontal theta dynamics, we defined an 8 mm radius spheres around the peak value of those regions sensitive to UPE and outcome valence within the mPFC – with the MarsBaR ROI toolbox. We extracted, for each of these regions, the average beta-slope from the outcome valence and UPE contrasts. Finally, stepwise linear regression analysis was used to assess the relationship between the fMRI measures and the beta-slopes extracted from the time-frequency analysis. The entry criterion was  $p < .05$  and the exit criterion was  $p > .10$ .

**Functional connectivity analysis.** For the functional connectivity analysis, an 8 mm radius ROI was defined around the peak value of the regions that were significantly sensitive to outcome valence and UPE. For each participant, the maximum peak within the ROI was analyzed. Individual time-courses from this ROI were extracted, and an extended model was built. This model included the conditions previously defined for the reversal learning task plus the extracted time-course and the derived *psychophysiological interaction* (PPI) from those regions within the standard PPI approach (Friston et al., 1997) as regressors. In particular, we used PPIs to test for higher inter-regional coupling with those regions sensitive to outcome valence and unsigned prediction error during outcome processing. The computed first level PPI results were taken to a second level one-sample t-test analysis. Results are reported at  $p < 0.05$  (FWE-corrected) at the peak level with a minimal cluster size of 2 voxels.

## RESULTS

**Behavior.** The participants had similar performance levels in both the EEG and the fMRI sessions. Paired t-test analyses showed no differences in % of correct responses ( $t(16) = .94, p = .36$ ) nor in the number of negative feedback before participants switch to the current correct response after a reversal ( $t(16) = 1.2, p = .24$ ). Indeed, there were high significant correlations between sessions for both % of correct responses ( $\rho(17) = .67; p = .003$ ) and negative feedback perseveration ( $\rho(17) = .80; p < .001$ ) (Fig. 2A,B).

Additionally, an RL model was fitted to participants' behavioral performance in order to estimate single-trial prediction errors (EEG session: Pseudo- $R^2 = .48$ ; SD = .10; fMRI session: Pseudo- $R^2 = .45$ , SD = .15; no differences between sessions,  $t < 1$ ). The learning rate ( $\rho(17) = .78, p < .001$ ) and the inverse of the temperature value ( $\rho(17) = .61, p = .01$ ), were highly correlated between sessions as well (Fig. 2C,D). These results show that participants used very similar strategies in both sessions, suggesting that similar neuronal mechanisms were engaged.

**Relationship between mid-frontal theta and both outcome valence and unsigned prediction error.** Similar to previous studies (Mas-Herrero et al., 2015; Marco-Pallares et al., 2008) the time-frequency analysis revealed a clear enhancement of theta activity (4-8 Hz) in positive and negative feedback with its maximum values between 200 and 400 ms after feedback onset (Fig 3A). Topographical maps indicated that the maximum effect was localized at FCz (Fig 3C).

In order to study whether mid-frontal theta activity within this time-frequency windows (averaged power from 200 to 400 msec, from 4 to 8 Hz at Fcz) was similarly modulated by unsigned prediction error following either positive or negative feedback, both types of feedback were split into 10 percentile groups (from 10<sup>th</sup> to 100<sup>th</sup>) derived from the individual distribution of UPE predicted on a trial-by-trial basis by the RL model (Fig 3B). These two effects, outcome valence (gain and loss) and UPE (10 levels), were included as within-participants factors in a Repeated

Measures ANOVA. The analysis revealed a main effect of outcome valence ( $F(1,16) = 45.11, p < .001$ ) and UPE ( $F(1,16) = 14.26, p < .001$ ). However, these two effects did not interact ( $F(1,16) = 1.2, p = .30$ ). That is, increases of mid-frontal theta activity were greater following negative than positive feedback but increased with unsigned prediction error independently of the outcome valence (Fig 3D). We also tested these effects on a trial-by-trial basis, performing a multiple-regression analysis with increases of mid-frontal theta activity – at FCz – as the dependent variable and outcome valence and UPE as independent variables. The beta values obtained, for both effects, were significantly different from 0, supporting the relationship between mid-frontal theta activity and these two variables, outcome valence ( $t(16) = 7.17; p < .001$ ) and UPE ( $t(16) = 4.79; p < .001$ ). Topographical distribution of the beta values of the two effects showed that its maximum value was at Fcz (Fig.3C).

**Spatial localization of outcome valence and UPE effects.** During the fMRI session, we found that the two main contrast – UPE and outcome valence – engaged the mPFC, but at different locations. Negative feedback, compared to positive, induced significant signal change mainly in the pre-Supplementary Motor Area (pre-SMA). In contrast, the dorsomedial Prefrontal Cortex (dmPFC) responded to variations of unsigned prediction errors. (Fig 4A; Table 1).

**Correlation between mid-frontal theta power and brain activity.** In order to assess the relationship between theta sensitivity to either outcome valence and UPE evaluation, on the one hand, and pre-SMA and dmPFC sensitivity, on the other, we performed stepwise linear regression analysis. Theta sensitivity to outcome valence evaluation was only predicted by pre-SMA changes to outcome valence ( $R^2 = 0.3, F(1,16) = 6.3, p = 0.02$ ). Conversely, individual differences in mid-frontal theta sensitivity to UPE was predicted by dmPFC sensitivity to UPE ( $R^2 = 0.32, F(1,16) = 7.01, p = 0.01$ ) (Fig. 5).

**Functional connectivity of regions sensitive to outcome valence and UPE.** We then wanted to determine whether these two regions, with dissociable impact into mid-frontal theta activity, were engaged into the same network or conversely, if they presented a different connectivity pattern. Functional connectivity analyses of these two sub-regions support the last hypothesis (Fig. 4B; table 2). The pre-SMA, sensitive to outcome valence, was mainly engaged with insula, putamen and substantia nigra, a network also known as the salience network (SN) (Seeley et al., 2007). On the other hand, the dmPFC was engaged in a network involving the right dorsolateral prefrontal cortex (dlPFC), the ventromedial prefrontal cortex (vmPFC), and the right parietal cortex (PC). This network has been previously identified as the Central Executive Network (CEN).

## **DISCUSSION**

In the present study we explored the relationship between mid-frontal theta activity and the brain structures associated with different aspect of outcome monitoring processes: outcome valence and unsigned prediction error. Seventeen participants performed a reversal learning task in two separate sessions in which EEG and fMRI were recorded. Present results confirm, with a new set of participants, our previous study (Mas-Herrero and Marco-Pallarés, 2013) showing that increases of mid-frontal theta (4-8 Hz) power activity at the same time window – from 200 to 400 msec after feedback onset – are sensitive to both variations of unsigned prediction error and the valence of the outcome. Additionally, individual differences in these two independent effects on mid-frontal theta power were predicted by the activity of two sub-regions of the mPFC. The pre-SMA sensitivity to outcome valence specifically predicted mid-frontal theta responses following negative compared to positive feedback. In contrast, individual differences in dmPFC sensitivity to UPE specifically predicted increases of mid-frontal theta power in response to variations of unsigned prediction error. Finally, these two sub-regions, with a differentiated effect on theta power increases, presented different functional connectivity profiles. While the pre-SMA was

functionally connected with regions of the SN, the dmPFC was engaged with a group of regions from the CEN. These results indicate the mid-frontal theta activity is not only reflecting activity of different mPFC sub-regions of one single network, but from different networks.

Previous intracranial studies, in both epilepsy human patients (Uchida et al., 2002; Nishida et al., 2004) and monkeys performing tasks involving executive functions and error processing (Tsujimoto et al., 2006; Womelsdorf et al., 2010) have consistently shown that mPFC is a generator of theta activity. Indeed, mid-frontal theta activity has been typically observed in situations involving the engagement of the mPFC, such conflict, uncertainty, prediction error, error and punishment (Nachev et al., 2005; Behrens et al., 2007). The ubiquity of this signal suggests that it may represent a common mechanism to temporally coordinate mPFC computations (Cavanagh et al., 2012). However, those computations may occur in functionally distinct subpopulations of neurons. For instance, neural recording studies have shown different mPFC's neuronal populations responding to either positive, negative or both prediction errors (Matsumoto et al., 2007). Similarly, fMRI studies have shown functional subdivisions within the mPFC, from dorsal-to-ventral to posterior-to-anterior gradients (Venkatraman et al., 2009; Taren et al., 2011; Bzdok et al., 2013) with dissociable connectivity profiles and functional roles (Seeley et al., 2007). The information encoded on each of these sub-regions and networks needs to be integrated to guide learning. For instance, our attention is increased by motivational salient events, and, at the same time, the identification of salient events might be influenced by the levels of attention (Menon and Uddin, 2010). Thus, theta might provide a temporal template to coordinate the spike timing of mPFC's sub-regions leading to coherent communication and serving as a fundamental mechanism to integrate information from functionally segregated sub-regions (Rony et al., 2008). Specifically, our results indicate that mid-frontal theta activity at the time of the outcome could provide a temporal window for the interaction of mPFC regions engaged with the SN and the CEN during feedback learning.

The SN and CEN together with the Default Mode Network (DMN) are critically involved in the control of attention and decision making. During the performance of cognitive-demanding tasks, the SN and the CEN typically show increases in activation (Sridharan et al., 2008). In contrast, the DMN presents the opposite pattern, decreasing its activation (Greicius et al., 2003). Previous studies have shown that SN and/or CEN may negatively regulate the DMN activity (Bonnelle et al., 2011; Chen et al., 2013). Interestingly, studies using EEG-fMRI approaches, at resting state, have shown a negative correlation between mid-frontal theta oscillations and the BOLD activity of regions from the DMN (Scheeringa et al., 2008; White et al., 2013). However, no previous studies have studied the relationship between mid-frontal theta power activity and brain activity in any of these networks while participants undergo a cognitive task. In contrast to the dynamic of mid-frontal theta activity observed at resting state, our results suggest that while performing a cognitive-demanding task, increases of mid-frontal theta activity at outcome delivery are positively modulated by regions from the SN and CEN. These findings indicate a similar activation pattern of these networks and their correlation with theta activity (that is a decrease of DMN activation with negative correlation with theta power and an increase of CEN and SN with positive theta correlation), suggesting a potential role of mid-frontal theta activity in the coordination of these networks.

The relationship between outcome valence effects on mid-frontal theta power activity and a region engaged with the SN agrees with previous studies suggesting that this effect may, in fact, reflect general salience processes rather than outcome value evaluation (Cavanagh et al., 2013). Indeed, a recent study has shown that in a real gambling situation in which the probability of obtaining a reward is very low and highly motivationally relevant, increases of mid-frontal theta power were greater in positive compared to negative feedback (Alicart et al., 2015). Similar findings have been described in the case of the Feedback Related Negativity (FRN) (Talmi et al., 2013), an Event-Related Potential also related to valence and prediction error processing with similar time course and topographical distribution to mid-frontal theta activity (Gehring and Willoughby,

2002). In parallel, our results are consistent with recent studies that have pointed out the role of the SMA and pre-SMA in the processing of motivationally relevant information, as errors and other salient signals (Litt et al., 2011; Bonini et al., 2014).

Additionally, our results further support the idea that increases of mid-frontal theta activity are also modulated by UPE. This surprise signal is consistent with attentional models of learning that suggest that unexpected outcomes may drive learning by increasing attention to subsequent events (Pearce and Hall, 1980). Notably, we have shown that such modulation is related to the engagement of an mPFC sub-region functionally connected with brain-structures from the CEN. The CEN plays an important role in sustaining attention, manipulating information from working memory and decision-making in goal directed behaviors (Miller and Cohen, 2001; Petrides, 2005; Koechlin and Summerfield, 2007). Similarly, increases of mid-frontal theta activity reflect task difficulty (Gevins et al., 1997) and increase with working memory load (Jensen and Tesche, 2002; Deiber et al., 2007). Therefore, the relationship reported in the present study, between mid-frontal theta activity increases due to attentional signals as unsigned prediction errors and a specific subregion of the mPFC, the dmPFC, functionally connected with the CEN, agree with a growing body of literature that has related mid-frontal theta activity with cognitive control and attention (Ridderinkhof et al., 2004). Interestingly, Hajihosseini et al. (2013) proposed a functional dissociation between “evoked” theta oscillatory activity power and induced oscillatory power, that is, the oscillatory activity subtracting the Event-Related Potentials (ERP) component. In this study, authors showed that the induced activity was associated to the probability of the outcomes, while the Feedback-Related Negativity (FRN) ERP responded to valence. In addition, Cohen et al. 2013 showed that conflict responses were driven mainly by non-phase locked (induced) oscillatory theta responses. One of the strengths of our study is the possibility to compute unsigned prediction error on a trial by trial bases using a reinforcement-learning computational model, but this complicates the differentiation between evoked and induced oscillatory responses. Indeed, the classical procedure to compute induced oscillatory activity (Cohen et al. 2013) is by

subtracting, for each condition, the event-related responses to single trial data. However, in our case, we do not have “conditions” for unsigned prediction error (as it is computed on each trial and presents continuous values) and therefore the subtraction of event-related responses for each condition is not possible. Future studies using different conditions for high and low prediction error (see e.g. Hajihosseini et al. 2012) might help in determining the evoked or induced nature of the theta oscillatory activity reported in the present manuscript.

The approach used in the present study combines information from brain electrical activity recorded using EEG and BOLD activity from fMRI. This approach takes advantage of the excellent spatial resolution of the fMRI and allows studying brain oscillatory activity using EEG data. The two sessions were separated 4 months in order to minimize re-test effects. A potential problem of this procedure would be differences in task performance between sessions (e.g., because participant used different strategies in the two sessions). However, in the present study, behavioral measures presented a very high reliability, suggesting that the strategy used by the participants in the two sessions was very similar, and supporting the idea that individual differences in the reversal learning task are highly consistent and might reflect a trait characteristic, as proposed in different studies (Jocham et al., 2009, den Oude et al., 2013 Padrao et al., 2015). Additionally, the use of two separate sessions allows us to adapt each session to the different technical requirements of each neuroimaging modality. Thus, the use of the approach implemented in this study may be convenient for processes that are highly consistent across time (for instance, cognitive flexibility, working memory processes, etc). However, a limitation of the present approach is that there are no direct recordings of the theta activity in the target areas. Future studies using intracranial recording could test whether electrodes placed into the dmPFC and the pre-SMA are sensitive to different aspect of outcome evaluation (surprise and outcome valence, respectively) within the theta range and whether the phase of theta cycles in these two electrodes is synchronized.

It is also important to note that the relationship between BOLD response and brain electrical activity (and, in concrete, oscillatory activity) is not well yet well understood. Some initial studies comparing Local Field Potentials and BOLD response found that that the strongest relationship between these two measures was in LFP high-frequency activity (gamma band), and that low oscillatory frequencies presented negative correlations (see e.g. Mukamel et al., 2005), but recent studies have revealed that this relationship might be more complex. For example, a recent study (Hipp et al., 2015) showed that resting state EEG correlation structure activity correlated to BOLD at a very wide oscillatory range (2-128 Hz), being this correlation strongest at alpha and beta activity. Regarding theta activity, Scheeringa et al., (2009) found a complex patter of positive and negative correlations of theta and alpha oscillatory activity with BOLD activity in a working memory task. Importantly, Kujala et al., (2014) found that the correlation between BOLD and MEG oscillatory activity varied as a function of the different brain regions activated in a reading paradigm. Therefore, visual cortex presented a pattern very similar to the one described in Mukamel et al., (2005), that is, positive correlation of BOLD activity with high (gamma-band) frequencies and inverse correlation with low (delta-, theta- and alpha-band) frequencies. In contrast, other brain areas presented very different patterns. For example, supra-temporal and inferior frontal areas presented positive correlations of BOLD activity with gamma, but also theta (6 Hz) and beta bands. All these studies point out to a rich and complex pattern of relationship between EEG/MEG and BOLD responses, which would depend on the brain region and function involved. In this regard, the positive correlation of BOLD and theta oscillatory activity found in the present study is fully compatible with (a) the well-known role of this oscillatory activity in cognitive control function (Cavanagh and Frank, 2014), (b) intracranial recording studies identifying the mPFC as a generator of mid-frontal theta oscillations in tasks involving cognitive control and error processing (Uchida et al., 2002, Nishida et al., 2004, Tsujimoto et al. 2006) and (c) fMRI studies observing the engagement of the mPFC following negative feedback (Ridderinkhof et al., 2004; Jocham et al., 2009).

In summary, our study shows that increases of mid-frontal theta activity at outcome delivery are influenced by the activity of at least two different sub-regions of the mPFC, the pre-SMA and dmPFC, which are functionally connected to the SN and CEN. Present results might indicate that mid-frontal theta activity serve as temporal context for the coordination of these networks during feedback learning.

**ACKNOWLEDGEMENTS.** Supported by Spanish Government grants (PSI2012-37472 to J. M. P.), and grants from the Catalan Government (2009-SGR-93) to J.M.P; and FPI to E. M. H. (BES-2010-032702). The authors declare no conflict of interest.

## **References**

- Alicart H., Cucurell D., Mas-Herrero E., Marco-Pallarés J., 2015. Human oscillatory activity in near-miss events. *Soc. Cog. Affec. Neurosci.* nsv033.
- Behrens T.E.J., Woolrich M.W., Walton M.E., Rushworth M.F.S., 2007. Learning the value of information in an uncertain world. *Nat. Neurosci.* 10, 1214–1221.
- Bonini F., Burle B., Liégeois-Chauvel C., Régis J., Chauvel P., Vidal F., 2014. Action monitoring and medial frontal cortex: leading role of supplementary motor area. *Science* 343, 888–891.
- Bonnelle V., Leech R., Kinnunen K.M., Ham T.E., Beckmann C.F., De Boissezon X., Greenwood R.J., Sharp D.J., 2011. Default mode network connectivity predicts sustained attention deficits after traumatic brain injury. *J. Neurosci.* 31, 13442–13451.
- Buzsáki G., Draguhn A., 2004. Neuronal oscillations in cortical networks. *Science* 304, 1926–1929.

Bzdok D., Langner R., Schilbach L., Engemann D.A., Laird A.R., Fox P.T., Eickhoff S.B., 2013. Segregation of the human medial prefrontal cortex in social cognition. *Front. Hum. Neurosci.* 7, 232.

Cavanagh J.F., Eisenberg I., Guitart-Masip M., Huys Q., Frank M.J., 2013. Frontal theta overrides pavlovian learning biases. *J. Neurosci.* 33, 8541–8548.

Cavanagh J.F., Figueroa C.M., Cohen M.X., Frank M.J., 2011. Frontal Theta Reflects Uncertainty and Unexpectedness during Exploration and Exploitation. *Cereb. Cortex.* bhr332.

Cavanagh J.F., Zambrano-Vazquez L., Allen J.J.B., 2012. Theta lingua franca: a common mid-frontal substrate for action monitoring processes. *Psychophysiology* 49, 220–238.

Cohen M.X., Wilmes K., Vijver I van de., 2011. Cortical electrophysiological network dynamics of feedback learning. *Trends Cogn. Sci.* 15, 558–566.

Cohen M.X., Donner T.H., 2013. Midfrontal conflict-related theta-band power reflects neural oscillations that predict behavior. *J Neurophysiol.* 110, 2752-2763.

Cools R., Clark L., Owen A.M., Robbins T.W., 2002. Defining the neural mechanisms of probabilistic reversal learning using event-related functional magnetic resonance imaging. *J Neurosci.* 22, 4563–4567.

Cools, R., Lewis, S. J., Clark, L., Barker, R. A., Robbins, T. W., 2007. L-DOPA disrupts activity in the nucleus accumbens during reversal learning in Parkinson's disease. *Neuropsychopharmacology* 32(1), 180-189.

Chase, H. W., Swanson, R., Durham, L., Benham, L., Cools, R., 2011. Feedback-related negativity codes prediction error but not behavioral adjustment during probabilistic reversal learning. *J. Cogn. Neurosci.* 23(4), 936-946.

Chen A.C., Oathes D.J., Chang C., Bradley T., Zhou Z-W., Williams L.M., Glover G.H., Deisseroth K., Etkin A., 2013. Causal interactions between fronto-parietal central executive and default-mode networks in humans. *Proc. Natl. Acad. Sci. USA* 110, 19944–19949.

Deiber M-P., Missonnier P., Bertrand O., Gold G., Fazio-Costa L., Ibañez V., Giannakopoulos P., 2007. Distinction between perceptual and attentional processing in working memory tasks: a study of phase-locked and induced oscillatory brain dynamics. *J. Cogn. Neurosci.* 19, 158–172.

den Ouden, H. E., Daw, N. D., Fernandez, G., Elshout, J. A., Rijpkema, M., Hoogman, M., Franke, B., Cools, R., 2013. Dissociable effects of dopamine and serotonin on reversal learning. *Neuron* 80(4), 1090-1100.

Fellows, L. K., Farah, M. J., 2003. Ventromedial frontal cortex mediates affective shifting in humans: evidence from a reversal learning paradigm. *Brain* 126(8), 1830-1837.

Friston K.J., Buechel C., Fink G.R., Morris J., Rolls E., Dolan R.J., 1997. Psychophysiological and modulatory interactions in neuroimaging. *Neuroimage* 6, 218–229.

Gehring W.J., Willoughby A.R., 2002. The medial frontal cortex and the rapid processing of monetary gains and losses. *Science* 295, 2279–2282.

Gevins A., Smith M.E., McEvoy L., Yu D., 1997. High-resolution EEG mapping of cortical activation related to working memory: effects of task difficulty, type of processing, and practice. *Cereb. Cortex* 7, 374–385.

Greicius M.D., Krasnow B., Reiss A.L., Menon V., 2003. Functional connectivity in the resting brain: a network analysis of the default mode hypothesis. *Proc. Natl. Acad. Sci. USA* 100, 253–258.

HajiHosseini A., Rodríguez-Fornells A., Marco-Pallarés J. 2012. The role of beta-gamma oscillations in unexpected rewards processing. *Neuroimage.* 60, 1678-1685

Hajihosseini A., Holroyd C.B., 2013. Frontal midline theta and N200 amplitude reflect complementary information about expectancy and outcome evaluation. *Psychophysiology.* 50, 550-562.

Hipp, J.F., Siegel, M., 2015. BOLD fMRI Correlation Reflects Frequency-Specific Neuronal Correlation. *Curr. Biol.* 25, 1368–1374

Jensen O., Tesche C.D., 2002. Frontal theta activity in humans increases with memory load in a working memory task. *Eur. J. Neurosci.* 15, 1395–1399.

Jocham, G., Klein, T. A., Neumann, J., von Cramon, D. Y., Reuter, M., Ullsperger, M., 2009. Dopamine DRD2 polymorphism alters reversal learning and associated neural activity. *J Neurosci.* 29(12), 3695-3704.

Koechlin E., Summerfield C., 2007. An information theoretical approach to prefrontal executive function. *Trends Cogn. Sci.* 11, 229–235.

Kujala, J., Sudre, G., Vartiainen, J., Liljeström, M., Mitchell, T., Salmenin, R., 2014. Multivariate analysis of correlation between electrophysiological and hemodynamic responses during cognitive processing. *NeuroImage* 92, 207–216

Litt A., Plassmann H., Shiv B., Rangel A., 2011. Dissociating valuation and saliency signals during decision-making. *Cereb. Cortex* 21, 95–102.

Marco-Pallares J., Cucurell D., Cunillera T., García R., Andrés-Pueyo A., Münte T.F., Rodríguez-Fornells A., 2008. Human oscillatory activity associated to reward processing in a gambling task. *Neuropsychologia* 46, 241–248.

Mas-Herrero E., Marco-Pallarés J., 2013. Frontal Theta Oscillatory Activity Is a Common Mechanism for the Computation of Unexpected Outcomes and Learning Rate. *J. Cogn. Neurosci.* 26(3), 447-458.

Mas-Herrero E., Ripollés P., HajiHosseini A., Rodríguez-Fornells A., Marco-Pallarés J., 2015. Beta oscillations and reward processing: Coupling oscillatory activity and hemodynamic responses. *Neuroimage* 119, 13–19.

Matsumoto M., Matsumoto K., Abe H., Tanaka K., 2007. Medial prefrontal cell activity signaling prediction errors of action values. *Nat. Neurosci.* 10, 647–656.

Menon V., Uddin L.Q., 2010. Saliency, switching, attention and control: a network model of insula function. *Brain. Struct. Funct.* 214, 655–667.

- Miller E.K., Cohen J.D., 2001. An integrative theory of prefrontal cortex function. *Annu. Rev. Neurosci.* 24, 167–202.
- Mukamel, R., Gelbard, H., Arieli, A., Hasson, U., Fried, I., Malach, R., 2005. Coupling between neuronal firing, field potentials, and fMRI in human auditory cortex. *Science* 309, 951–954.
- Nachev P., Rees G., Parton A., Kennard C., Husain M., 2005. Volition and conflict in human medial frontal cortex. *Curr. Biol.* 15, 122–128.
- Nishida, M., Hirai, N., Miwakeichi, F., Maehara, T., Kawai, K., Shimizu, H., Uchida, S., 2004. Theta oscillation in the human anterior cingulate cortex during all-night sleep: an electrocorticographic study. *J. Neurosci. Res.* 50, 331–341
- Padrao, G., Mallorquí, A., Cucurell, D., & Rodriguez-Fornells, A., 2015. Individual differences in error tolerance in humans: Neurophysiological evidences. *Cogn. Affect. Behav. Neurosci.* 15(4), 808-821.
- Pearce J.M., Hall G., 1980. A model for Pavlovian learning: variations in the effectiveness of conditioned but of unconditioned stimuli. *Psychological Review* 87, 532-552.
- Petrides M., 2005. Lateral prefrontal cortex: architectonic and functional organization. *Philos Trans. R. Soc. Lond.* 360, 781–795.
- Philiastides, M. G., Biele, G., Vavatzanidis, N., Kazzner, P., Heekeren, H. R., 2010. Temporal dynamics of prediction error processing during reward-based decision making. *NeuroImage* 53(1), 221-232.
- Ridderinkhof K.R., Ullsperger M., Crone E.A., Nieuwenhuis S., 2004. The role of the medial frontal cortex in cognitive control. *Science* 306, 443–447.
- Rony P., Bauer E.P., Paré D., 2008. Theta synchronizes the activity of medial prefrontal neurons during learning. *Learning & Memory* 15(7), 524-531.

Scheeringa R., Bastiaansen M.C.M., Petersson K.M., Oostenveld R., Norris D.G., Hagoort P., 2008. Frontal theta EEG activity correlates negatively with the default mode network in resting state. *Int. J. Psychophysiol.* 67, 242–251.

Scheeringa, R., Petersson, K.M., Oostenveld, R., Norris, D.G., Hagoort, P., Bastiaansen, M.C.M., 2009. Trial-by-trial coupling between EEG and BOLD identifies networks related to alpha and theta EEG power increases during working memory maintenance. *NeuroImage* 44, 1224–1238.

Seeley W.W., Menon V., Schatzberg A.F., Keller J., Glover G.H., Kenna H., Reiss A.L., Greicius M.D., 2007. Dissociable intrinsic connectivity networks for salience processing and executive control. *J. Neurosci.* 27, 2349–2356.

Sridharan D., Levitin D.J., Menon V., 2008. A critical role for the right fronto-insular cortex in switching between central-executive and default-mode networks. *Proc. Natl. Acad. Sci. USA* 105, 12569–12574.

Talmi D., Atkinson R., El-Deredy W., 2013. The feedback-related negativity signals salience prediction errors, not reward prediction errors. *J. Neurosci.* 33, 8264–8269.

Taren A.A., Venkatraman V., Huettel S.A., 2011. A parallel functional topography between medial and lateral prefrontal cortex: evidence and implications for cognitive control. *J. Neurosci.* 31, 5026–5031.

Tsujimoto, T., Shimazu, H., Isomura, Y., 2006. Direct Recording of Theta Oscillations in Primate Prefrontal and Anterior Cingulate Cortices. *J. Neurophysiol.* 95, 2987–3000

Uchida, S., Maehara, T., Hirai, N., Kawai, K., Shimizu, H., 2003.  $\alpha$  Oscillation in the anterior cingulate and  $\beta$ -1 oscillation in the medial temporal cortices: a human case report. *J. Clin. Neurosci.* 10, 371–374

Ullsperger M., Danielmeier C., Jocham G., 2014. Neurophysiology of performance monitoring and adaptive behavior. *Physiological reviews* 94(1), 35-79.

Venkatraman V., Rosati A.G., Taren A.A., Huettel S.A., 2009. Resolving response, decision, and strategic control: evidence for a functional topography in dorsomedial prefrontal cortex. *J. Neurosci.* 29, 13158–13164.

Watkins C.J.C.H, Dayan P., 1992. Q-learning. *Machine Learning* 8, 279–292.

White T.P., Jansen M., Doege K., Mullinger K.J., Park S.B., Liddle E.B., Gowland P.A., Francis S.T., Bowtell R., Liddle P.F., 2013. Theta power during encoding predicts subsequent-memory performance and default mode network deactivation. *Hum. Brain Mapp.* 34, 2929–2943.

Womelsdorf T., Schoffelen J-M., Oostenveld R., Singer W., Desimone R., Engel A.K., Fries P., 2007. Modulation of neuronal interactions through neuronal synchronization. *Science* 316, 1609–1612.

Womelsdorf, T., Johnston, K., Vinck, M., Everling, S., 2010. Theta-activity in anterior cingulate cortex predicts task rules and their adjustments following errors. *Proc. Natl. Acad. Sci. USA* 107, 5248–5253

Cavanagh, J. F., Frank, M. J., 2014. Frontal theta as a mechanism for cognitive control. *Trends Cogn. Sci.*, 18(8), 414-421.

<b>fMRI UPE effect</b>			
<b>Anatomical Area</b>	<b>Coordinates</b>	<b>Size</b>	<b>t-value</b>
Middle Occipital Gyrus	-14 -97 2	3	7,38
Dorsomedial Prefrontal Cortex	1 27 46	2	7,24

<b>fMRI Valence effect</b>			
<b>Anatomical Area</b>	<b>Coordinates</b>	<b>Size</b>	<b>t-value</b>
Left Middle Occipital Gyrus; Left Superior Occipital Gyrus; Left Calcarine Gyrus	-11 -97 2	48	9,54
Pre-Supplementary Motor Area	5 12 54	21	9,51

**Table 1. Effects of UPE and outcome valence on fMRI signal**

Enhanced group level fMRI-signals for the UPE and outcome valence contrasts thresholded at a FWE  $p < 0.05$  with 2 voxels of cluster extent (see also Fig. 2A). MNI coordinates are used.

<b>Pre-SMA seed</b>				
<b>Anatomical Area</b>	<b>Coordinates</b>	<b>Size</b>	<b>t-value</b>	
Left Dorsolateral Prefrontal Cortex	-52 4 18	34	9,92	
Left Inferior Parietal Gyrus; Left Supramarginal Gyrus	-59 -56 42	39	9,77	
Pre-Supplementary Motor Area; Dorsomedial Prefrontal Cortex	8 4 62	102	9,36	
Right Putamen; Right Insula; Right Pallidum; Right Caudate	23 8 2	101	9,10	
Left Putamen; Left Insula; Left Pallidum; Left Caudate	-18 12 2	91	9,06	
Right Inferior Orbitofrontal Cortex	42 42 -6	38	8,89	
Left Inferior Orbitofrontal Cortex	-48 42 2	27	8,41	
Substantia Nigra; Thalamus	12 -18 -6	25	7,99	
<b>dmPFC seed</b>				
<b>Anatomical Area</b>	<b>Coordinates</b>	<b>Size</b>	<b>t-value</b>	
Dorsomedial Prefrontal Cortex; Left pre-Supplementary Motor Area; Right Middle Cingulum Gyrus	1 23 46	127	15,48	
Right Dorsolateral Prefrontal Cortex	42 12 46	138	12,67	
Left Insula	-29 23 -6	22	10,23	
Right Inferior Orbitofrontal Cortex; Right Insula	27 27 -6	32	10,00	
Left Middle Orbitofrontal Cortex; Left Middle Frontal Gyrus	-41 46 6	53	9,90	
Right Middle Frontal Gyrus; Right Superior Frontal Gyrus	35 57 6	48	8,87	
Right Inferior Parietal Gyrus; Right Supramarginal Gyrus	53 -60 42	82	8,32	

**Table 2. Changes in interregional functional connectivity of the fMRI-data**

Local maxima for the functional coupling with the pre-SMA and dmPFC seeds specifically testing for higher coupling in the context of outcome monitoring respect the implicit baseline. Results are reported at  $p < 0.05$  FWE corrected threshold at the peak level with 2 or more voxels of cluster extent (see also Fig. 2B). MNI coordinates are used.

**Figure**

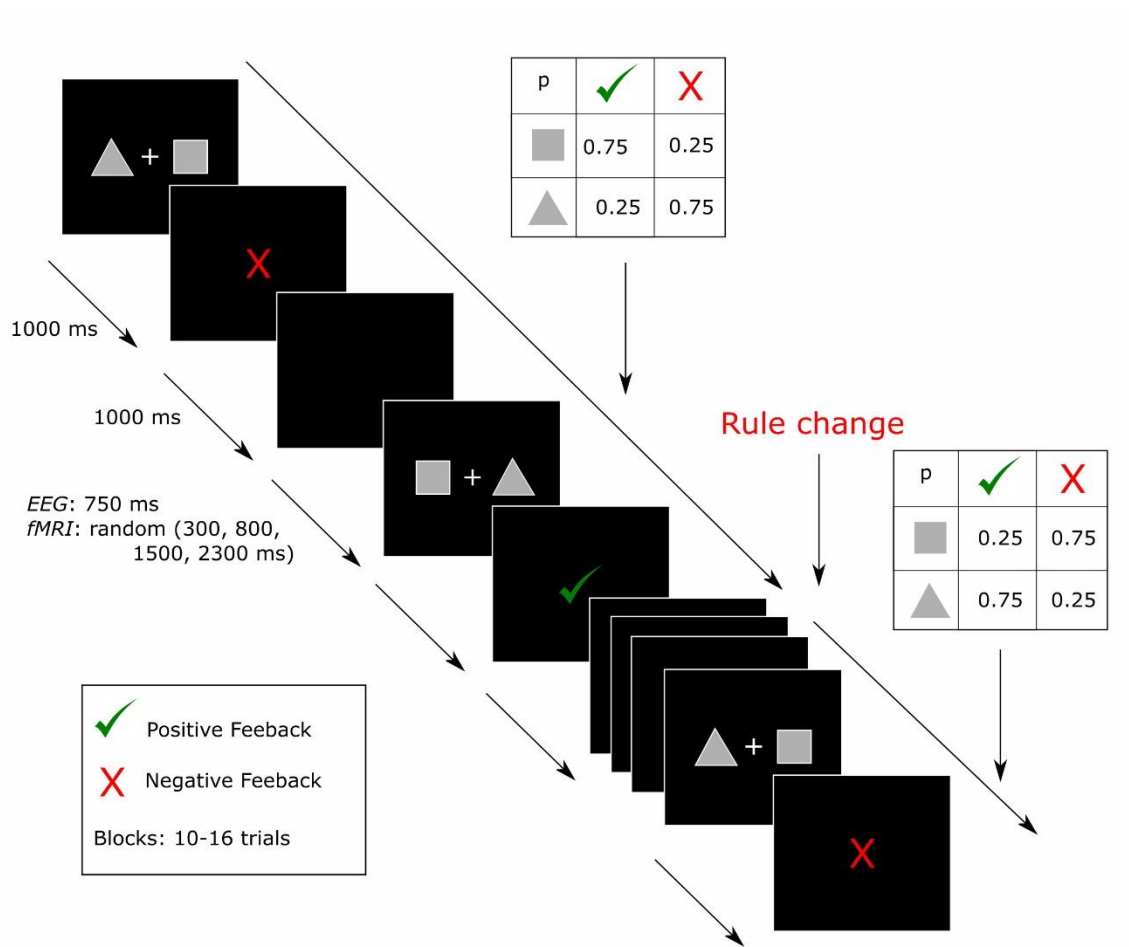


**Figure 1.** Task design. In each trial, two figures (a square and a triangle) appeared in the screen and the participants had to choose one of them. Then a feedback appeared, indicating whether participant had won or lost 4 cents. One figure had a probability of gain of 0.75, while the other had a winning probability of 0.25. Each 10-16 trials, and without informing the participant, the rule changed.

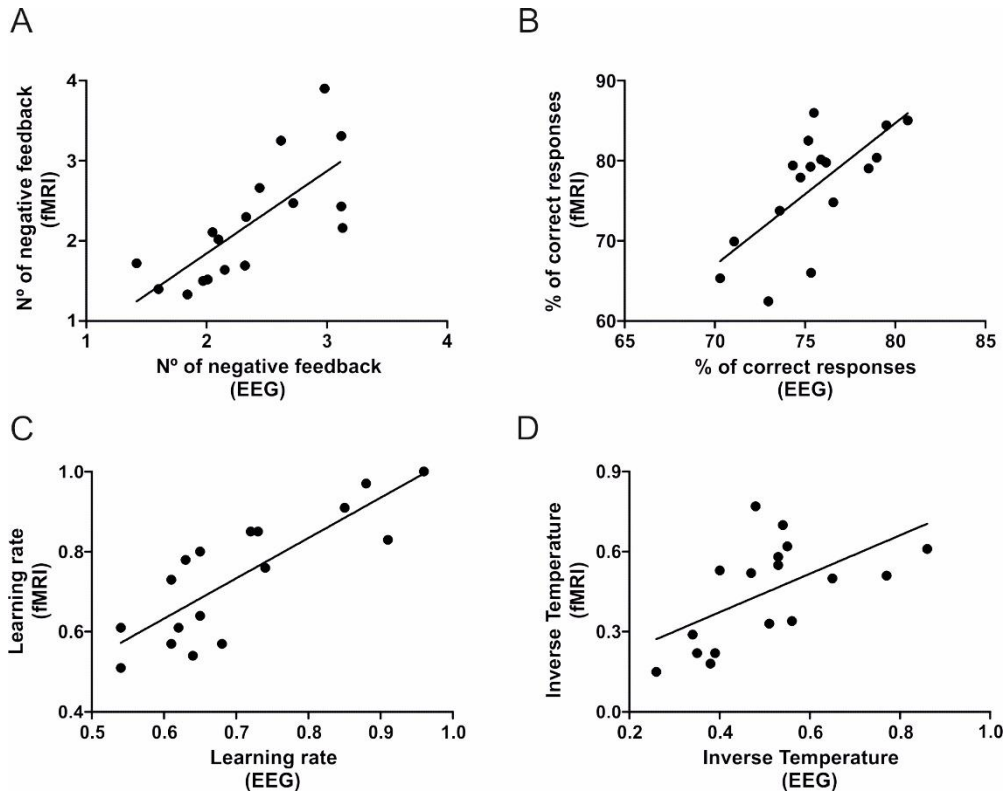


**Figure 2.** Behavioral correlation between the EEG and the fMRI session in the: A) number of negative feedback before participant performed a switch after a reversal; B) % of correct responses; C) learning rate and D) the inverse temperature derived from the RL model.

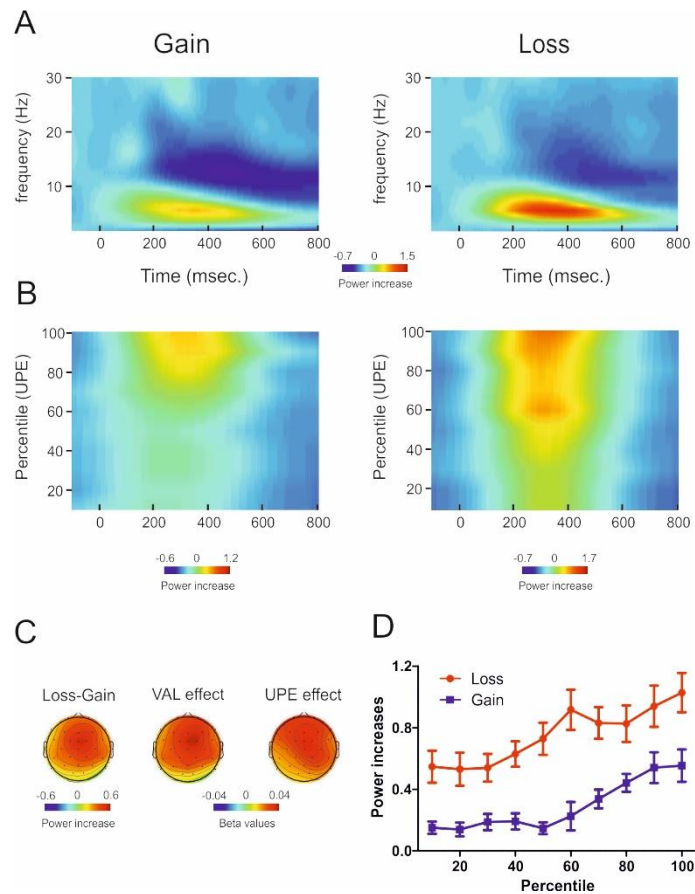
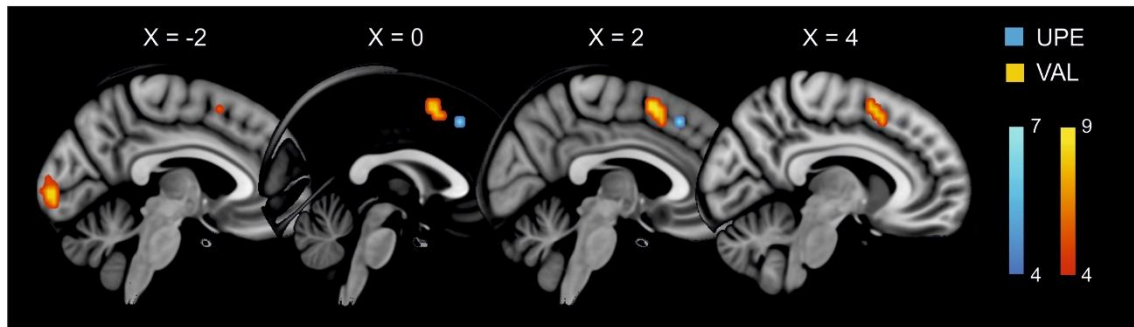


**Figure 3.** EEG results. A) Changes in power at FCz with respect to baseline (100 msec before feedback onset) after positive (left) and negative feedback (right). B) Variations in theta power (4-8Hz) at FCz due to UPE for both positive and negative feedback. C) Scalp maps for the difference in theta activity between loss and gain conditions and the distribution of beta values of UPE and VAL effects from the multiple regression analysis. D) Theta power responses to different degrees of UPE after positive and negative feedback. Although there is a clear increase of theta activity in negative compared to positive feedback, in both cases mid-frontal theta also increased with UPE.

A. Outcome valence and UPE effects on fMRI signal



B. Changes in interregional functional connectivity of fMRI data

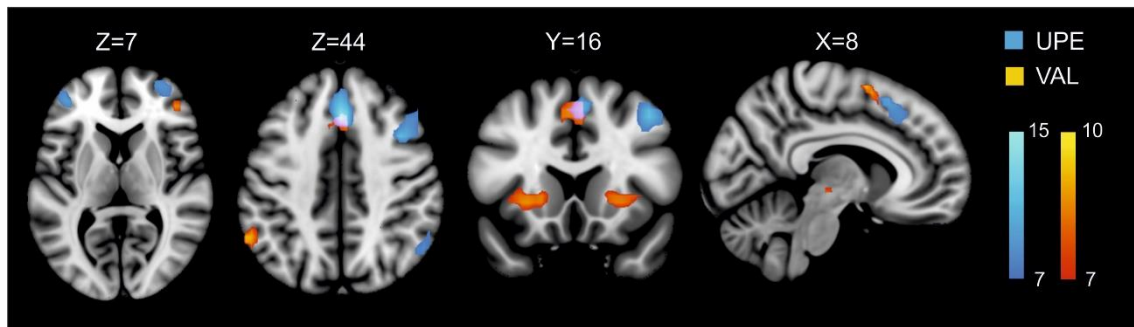


**Figure 4.** fMRI results. A) Outcome valence (VAL) and UPE effects on BOLD activity. Both effects peaked in the mPFC, however, VAL effect was more posterior than the UPE B) Functional connectivity of the two mPFC sub-regions identified as sensitive to outcome valence and UPE in the context of outcome processing. Note that the spatial dissociation found in the fMRI revealed a different pattern of connectivity.

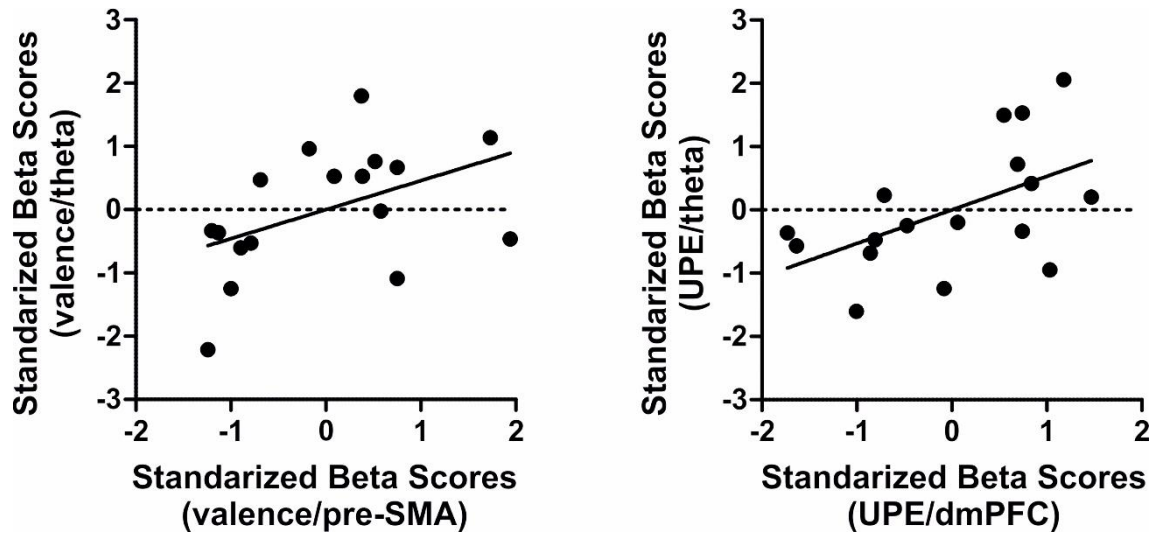


**Figure 5.** EEG-fMRI relationship A) Standardized beta scores from the multiple linear regression analysis performed to predict mid-frontal theta increases driven by outcome valence (left) and UPE (right). Note that pre-SMA activity from the fMRI outcome valence contrast specifically predicted individual differences of mid-frontal theta activity driven by the valence of the outcome. On the other hand, dmPFC activity from the UPE contrast predicted variations of mid-frontal theta activity driven by differences in UPE. B) Scatter plot of the relationship between increases of mid-frontal theta activity driven by outcome valence (left) and UPE (right) and activity of the pre-SMA (left) and the dmPFC (right).